ELSEVIER

Journal of Fluids and Structures 19 (2004) 277–289

JOURNAL OF FLUIDS AND STRUCTURES

www.elsevier.nl/locate/jnlabr/yjfls

Numerical simulation and experimental study of water entry of a wedge in free fall motion

G.X. Wu[a,*], H. Sun[b], Y.S. He[b]

[a] *Department of Mechanical Engineering, University College London, Torrington Place, London WC1E 7JE, UK*
[b] *Department of Engineering Mechanics, Shanghai Jiaotong University, Shanghai 20030, China*

Received 23 January 2003; accepted 5 January 2004

Abstract

The hydrodynamic problem of a two-dimensional wedge entering water through free fall motion is analysed based on the velocity potential theory. The gravity effect on the flow is ignored as our interest is over a short period of time. When the tip of the wedge touches water the flow is assumed to be similar. The problem of this similarity flow is solved by a boundary element method together with an analytical solution for the jet based on the shallow water approximation. This is then used as the initial condition for the subsequent solution which is obtained by the same boundary element method in a stretched coordinate system together with the time marching technique to follow the body motion and the free surface deformation. An auxiliary function is introduced to decouple the mutual dependence of the hydrodynamic force and the body acceleration. Experimental study is also undertaken. The numerical predication is found to be in good agreement with the measured data for wedges with different weight, dead-rise angle and entry speed.

1. Introduction

Water entry is part of the general fluid/structure impact problem. The first complete solution was obtained by Dobrovol'skaya (1969) for a two-dimensional wedge, based on velocity potential theory. The gravity effect was ignored and the entry speed was assumed to be constant. This led to a self-similar solution. By using the complex potential and conformal mapping, Dobrovol'skaya was able to transform the problem into an integral equation for a function $f(t)$ between $0 \leqslant t \leqslant 1$ and the result for pressure and velocity could then be obtained once the solution for this function was found. The same problem was reconsidered by Zhao and Faltinsen (1993). They calculated $f(t)$ using a refined procedure with a more advanced computer. In addition, they also used a boundary element method and solved the problem in the time domain. The results from these two methods were found to be in excellent agreement. There are also many other publications for the wedge problem based on the various simplified methods or asymptotic expansions. They include those by Greenhow (1987), Cointe (1991), Howison et al. (1991), Fraenkel and Mcleod (1997) and Mei et al. (1999). A related problem is that a wedge floating on the water surface starts moving downwards suddenly. Iafrati and Korobkin (2002) obtained a solution based on the small time expansion.

All these studies are, however, for body entry at a constant entry speed, which is rarely the case in reality. In this paper, the problem of a body entering water through free fall motion is considered. Such a 'minor' change leads to several extra difficulties: (i) the flow is no longer similar, which means the procedure of Dobrovol'skaya (1969) and many other mathematical approaches are no longer applicable, (ii) the body acceleration is unknown before the

*Corresponding author. Tel.: +44-20-7679-3870; fax: +44-20-7679-7065.
E-mail address: gx_wu@meng.ucl.ac.uk (G.X. Wu).

0889-9746/$ - see front matter © 2004 Elsevier Ltd. All rights reserved.
doi:10.1016/j.jfluidstructs.2004.01.001

solution for the fluid flow is found, which in turn depends on the acceleration and (iii) the pressure is no longer a by-product as in the constant speed problem and its accuracy will be fed back through the fluid flow via the calculation of the body acceleration. The last point is by no means trivial. In fact, it was observed by Zhao and Faltinsen (1993) that, although their overall results were excellent, there was a small area near the intersection of the body surface and the free surface, where the result for pressure is quite oscillatory. This behaviour does not affect their analysis because for a rigid body moving at a given speed, the pressure is not used in the calculation to obtain the body acceleration or the body deformation. In the work by Lu et al. (2000) in which the elastic body deformation is included, they showed that care is needed with the accuracy of the result for pressure. Inaccurate pressure can cause false structural deformation, which may subsequently lead to large error in solution for the flow. The problem is further complicated by the possibility of discontinuity of pressure in the fluid (Wu, 2001). Therefore, it is part of the aim of this work to overcome these difficulties and predict the body acceleration and the fluid flow accurately.

Water entry with nonconstant speed has been considered in a number of publications. Through an approximation and matching between the inner solution and outer solution, Faltinsen (2002) extended his equation for constant speed to variable speed, but no result is given. Iafrati et al. (2000) considered the nonlinear coupling between the force and the body acceleration through both explicit and implicit schemes. The former scheme uses the acceleration at the last time step to calculate the force at the current step. No details are spelled out for the implicit scheme. Here we adopt the method of using the auxiliary functions developed by Wu and Eatock Taylor (1996, 2003), which allows one to work out the body acceleration before the force is found.

In addition to the numerical solution, experiments are also performed with wedge of different weights, entry speeds and dead-rise angles. Measurement is made for the body acceleration and the body deformation. But in this paper, the analysis will focus on the former and no results for the deformation will be discussed.

2. Numerical simulation

2.1. Governing equations and boundary conditions

We consider the hydrodynamic problem due to a two-dimensional wedge with dead-rise angle β entering the water surface through free fall motion, as shown in Fig. 1. A Cartesian coordinate system $O-xy$ is defined in which y coincides with the symmetry line of the wedge and points vertically upwards, and the origin of the system is on the mean free surface. The fluid is assumed to be incompressible and inviscid, and the flow is assumed to be irrotational. A velocity potential ϕ can then be introduced, which satisfies the Laplace equation

$$\nabla^2\phi = 0 \tag{1}$$

in the fluid domain R. On the body surface S_0, we have

$$\frac{\partial\phi}{\partial n} = -Vn_y, \tag{2}$$

where V is the velocity of the body and is positive when the body moves downwards, and $\boldsymbol{n} = (n_x, n_y)$ is the normal vector of the body surface pointing out of the fluid domain. The kinematic and dynamic conditions on the free surface

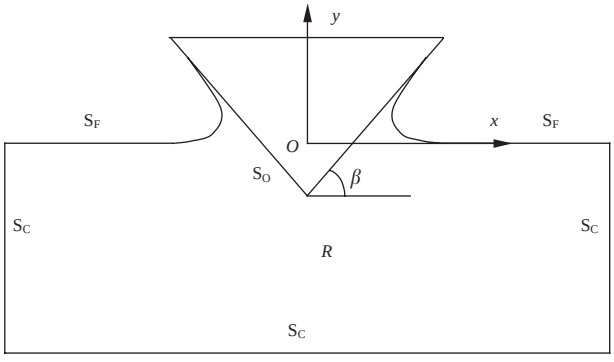

Fig. 1. Sketch of the problem.

S_F or $y = \eta$ can be written as

$$\frac{\partial \phi}{\partial y} = \frac{\partial \eta}{\partial t} + \frac{\partial \phi}{\partial x}\frac{\partial \eta}{\partial x}, \tag{3}$$

$$\frac{\partial \phi}{\partial t} + \frac{1}{2}\nabla\phi\nabla\phi = 0, \tag{4}$$

in which the effect due to the gravity on fluid flow has been ignored, as the impact lasts only for a very short period of time and the effect is of the second order based on small time expansion (Korobkin and Wu, 2000). The Lagrangian form of these two equations can be written as

$$\frac{\mathrm{d}\phi}{\mathrm{d}t} = \phi_t + \nabla\phi\nabla\phi = \frac{1}{2}\nabla\phi\nabla\phi, \tag{5}$$

$$\frac{\mathrm{d}x}{\mathrm{d}t} = \phi_x, \quad \frac{\mathrm{d}y}{\mathrm{d}t} = \phi_y. \tag{6}$$

2.2. Similarity solution at constant speed

In the time marching method, the solution of Eqs. (1)–(4) usually starts by assuming a tiny area near the tip of the wedge is already in the water and the free surface is initially flat and the potential on the free surface is zero. The reality is, however, that as soon as the tip of wedge touches water, the free surface begins to deform. If the entry speed is constant, the free surface shape remains unchanged, although its disturbed size increases with time. Thus, the initial solution based on the above procedure is not accurate. Such an inaccuracy is, however, found to have negligible effect on the solution at later time if the entry speed is constant. In fact the work by Lu et al. (2000) showed that the numerical result is in good agreement with the similarity solution (Dobrovol'skaya, 1969) after some initial stage. For a body in free fall, an initial error in the fluid flow may give wrong results for the force, which can in turn give the wrong results for the acceleration. Indeed, the numerical simulation in this work based on this procedure has showed that the force and acceleration histories have many sharp spikes.

Therefore, it is decided that the initial flow should be obtained from the similarity solution. When V is constant, the velocity potential has the form (Dobrovol'skaya, 1969)

$$\phi(x, y, t) = V^2 t\varphi(\tilde{\xi}, \tilde{\eta}) \tag{7}$$

where $\tilde{\xi} = x/Vt$ and $\tilde{\eta} = y/Vt$. Here $\varphi(\tilde{\xi}, \tilde{\eta})$ satisfies the Laplace equation in the coordinate system $(\tilde{\xi}, \tilde{\eta})$. The boundary conditions in Eqs. (2)–(4) become

$$\frac{\partial \varphi}{\partial n} = -\frac{\partial \varphi}{\partial \tilde{\xi}}\sin\beta + \frac{\partial \varphi}{\partial \tilde{\eta}}\cos\beta = -\cos\beta \tag{8}$$

on the body surface $\tilde{\eta} = -1 + \tilde{\xi}\tan\beta$, and

$$\varphi_{\tilde{\eta}} - \tilde{\eta}_{\tilde{\xi}}\varphi_{\tilde{\xi}} + \tilde{\xi}\tilde{\eta}_{\tilde{\xi}} - \tilde{\eta} = 0, \tag{9}$$

$$\varphi - \tilde{\xi}\varphi_{\tilde{\xi}} - \tilde{\eta}\varphi_{\tilde{\eta}} + 0.5(\varphi_{\tilde{\xi}}^2 + \varphi_{\tilde{\eta}}^2) = 0 \tag{10}$$

on the free surface $\tilde{\eta} = \tilde{\eta}(\tilde{\xi})$. It should be noted that Eq. (8) is imposed with $-1 \leqslant \tilde{\eta} \leqslant \tilde{\eta}_c$ where $(\tilde{\xi}_c, \tilde{\eta}_c)$ is the intersection point of the free surface with the wedge, which is to be found as part of the solution.

The free surface boundary conditions in Eqs. (9) and (10) are written based on an Eulerian description of the flow. This is quite effective when the free surface elevation $\tilde{\eta}(\tilde{\xi})$ is a single valued function. For the wedge problem, it is obviously not the case. Thus, through rotating the system $O{-}\tilde{\xi}\tilde{\eta}$ clockwise by an angle of $\pi/2 - \beta$, we introduce

$$\hat{\xi} = \tilde{\xi}\sin\beta - \tilde{\eta}\cos\beta, \quad \hat{\eta} = \tilde{\xi}\cos\beta + \tilde{\eta}\sin\beta. \tag{11}$$

In this new system, $\hat{\eta}$ is along the wedge surface. It can be verified that Eqs. (9) and (10) have the same form in the new system (in fact, the form of kinematic and dynamic conditions in this case should not depend on the orientation of the Cartesian system). An added advantage of this system is that for a fixed $\hat{\xi}$, $\hat{\eta}$ will just move in the direction of the wedge surface when the Euler form of the free surface boundary condition is used. No fluid particle will therefore move into the body because of numerical error.

Because of the nonlinearity in Eqs. (9) and (10), the problem may have to be solved through iteration. One way to do that is to assume an initial value for $\hat{\eta}(\hat{\xi})$ and φ on the free surface. Once the solution is found, Eqs. (9) and (10) will give new values for $\hat{\eta}(\hat{\xi})$ and φ on the free surface. This can be repeated until convergence is achieved. It is found, however,

that when a large computational domain is chosen, a large $\hat{\xi}$ in the equations will amplify the error in $\hat{\eta}_{\hat{\xi}}$ and $\varphi_{\hat{\xi}}$. This could lead to divergence of the result. Thus Eq. (9) is written as

$$\hat{\eta} - \hat{\xi}\hat{\eta}_{\hat{\xi}} = \varphi_{\hat{\eta}} - \hat{\eta}_{\hat{\xi}}\varphi_{\hat{\xi}}.$$

If we treat the right-hand side of this equation as known, it becomes a first-order ordinary differential equation for $\hat{\eta}$. Its solution can be written as

$$\hat{\eta} = -\hat{\xi}\left(\int_{\hat{\xi}_0}^{\hat{\xi}} \frac{\hat{\varphi}_{\hat{\eta}} - \hat{\eta}_{\hat{\xi}}\varphi_{\hat{\xi}}}{\hat{\xi}^2}\,\mathrm{d}\hat{\xi} - \frac{\hat{\eta}_0}{\hat{\xi}_0}\right), \tag{12}$$

where $(\hat{\xi}_0, \hat{\eta}_0)$ is the intersection point of the free surface and truncated boundary in the far field; their values can be worked out by the known x_0 and the assumption of $y_0 = 0$ (the free surface in the far field is assumed undisturbed). Eq. (10) can be dealt with in a similar manner. But it should be noted that

$$\frac{\partial\varphi[\hat{\xi}, \hat{\eta}(\hat{\xi})]}{\partial\hat{\xi}} = \varphi_{\hat{\xi}} + \varphi_{\hat{\eta}}\hat{\eta}_{\hat{\xi}}.$$

Thus, Eq. (10) can be written as

$$\begin{aligned}\varphi - \hat{\xi}\frac{\partial\varphi}{\partial\hat{\xi}} &= -\hat{\xi}\hat{\eta}_{\hat{\xi}}\varphi_{\hat{\eta}} + \hat{\eta}\varphi_{\hat{\eta}} - 0.5(\varphi_{\hat{\xi}}^2 + \varphi_{\hat{\eta}}^2)\\ &= -\hat{\eta}_{\hat{\xi}}\varphi_{\hat{\xi}}\varphi_{\hat{\eta}} - 0.5(\varphi_{\hat{\xi}}^2 - \varphi_{\hat{\eta}}^2)\end{aligned}$$

or

$$\varphi[\hat{\xi}, \hat{\eta}(\hat{\xi})] = \hat{\xi}\int_{\hat{\xi}_0}^{\hat{\xi}} \frac{\hat{\eta}_{\hat{\xi}}\varphi_{\hat{\xi}}\varphi_{\hat{\eta}} + 0.5(\varphi_{\hat{\xi}}^2 - \varphi_{\hat{\eta}}^2)}{\hat{\xi}^2}\,\mathrm{d}\hat{\xi} \tag{13}$$

under the assumption of $\varphi(\hat{\xi}_0, \hat{\eta}_0) = 0$. Eqs. (12) and (13) are then used for iteration. It is found that they lead to more stable results and faster convergence, although an under-relaxation coefficient is needed at small β.

When a very thin jet is developed, the numerical solution in the main region can be matched with an analytical approximation based on the shallow water theory in the jet zone. We may write [e.g., Mei (1983, Chapter 11)]

$$\varphi(\hat{\xi}, \hat{\eta}) = \sum_{n=0}^{\infty} \hat{\xi}^n \varphi_n(\hat{\eta}) \tag{14}$$

in the system defined in Eq. (11). Because the jet is usually very thin, two terms in the above equation would be sufficient. From Eq. (8), we have

$$\varphi_1 = \cos\beta. \tag{15}$$

Eq. (10) then gives

$$\varphi_0 - \hat{\eta}\varphi_{0\hat{\eta}} + 0.5(\cos^2\beta + \varphi_{0\hat{\eta}}^2) = 0$$

Differentiating with respect to $\hat{\eta}$, we obtain

$$\varphi_{0\hat{\eta}\hat{\eta}}(\varphi_{0\hat{\eta}} - \hat{\eta}) = 0.$$

The last two equations give $\varphi_0 = 0.5(\hat{\eta}^2 - \cos^2\beta)$ or $\varphi_0 = C\hat{\eta} - 0.5(C^2 - \cos^2\beta)$. Substituting the first of these two solutions into (9), the shape of the jet becomes $\hat{\xi} = \cos\beta$. This is in fact the surface of the wedge and therefore the solution is not physical. Substituting the second equation into (9) leads to a linear jet shape $\hat{\eta} = B(\hat{\xi} - \cos\beta) + C$ which is the desired solution.

In the numerical solution, we assume that the jet starts from a point at $(\hat{\xi}_s, \hat{\eta}_s)$ which can be decided by the thickness of the jet or the angle between the jet and the body surface. The potential at this point is assumed as φ_s. For the reason described above, we can write

$$\varphi = \cos\beta(\hat{\xi} - \hat{\xi}_s) + A(\hat{\eta} - \hat{\eta}_s) + \varphi_s, \tag{16}$$

$$\hat{\eta} = B(\hat{\xi} - \hat{\xi}_s) + \hat{\eta}_s. \tag{17}$$

Eq. (10) then gives

$$A = \hat{\eta}_s + \sqrt{\hat{\eta}_s^2 - (2\phi_s - 2\hat{\xi}_s\cos\beta + \cos^2\beta)}$$

and (9) gives

$$B = \frac{\hat{\eta}_s - A}{\hat{\xi}_s - \cos\beta}.$$

Using Eq. (17) at the intersection ($\hat{\xi}_c = \cos\beta, \hat{\eta}_c$) or the tip of the jet, we obtain $A = \hat{\eta}_c$. Subsequently, we have

$$\varphi_c = 0.5(\hat{\xi}_c^2 + \hat{\eta}_c^2), \tag{18}$$

which links the values of the potential at the intersection and its coordinates.

When a jet is developed during the iteration, $\hat{\xi}_s$ can be specified, and $\hat{\eta}_s$ and φ_s can be obtained from Eqs. (12) and (13). From Eqs. (16)–(18) the entire solution in the jet is then known and it will enter next iteration similar to the known boundary conditions. Once the next iteration is completed, a new $\hat{\xi}_s$ can be specified, and Eqs. (12) and (13) can give a new $\hat{\eta}_s$ and φ_s. The jet is then modified and a new iteration can start. This can be repeated until convergence has been achieved. The advantage of this procedure is that it can maintain the full jet no matter how long or how thin it is, and there is no extra computational effort for doing so, because the solution in the jet is already known at each iteration.

2.3. Time domain solution for wedge in free fall

When the speed of the body is not constant, the similarity solution written in terms of Eq. (7) is no longer valid. But we may write

$$\phi(x, y, t) = s\varphi(\tilde{\xi}, \tilde{\eta}, t), \tag{19}$$

where

$$s = \int_0^t V(\tau)\,\mathrm{d}\tau, \quad \tilde{\xi} = x/s, \quad \tilde{\eta} = y/s, \tag{20}$$

$\varphi(\tilde{\xi}, \tilde{\eta}, t)$ satisfies the Laplace equation in the coordinate system $(\tilde{\xi}, \tilde{\eta})$. On the free surface, the Lagrangian form of the boundary conditions can be written as

$$\frac{\mathrm{d}(s\tilde{\xi})}{\mathrm{d}t} = \varphi_{\tilde{\xi}}, \quad \frac{\mathrm{d}(s\tilde{\eta})}{\mathrm{d}t} = \varphi_{\tilde{\eta}}, \tag{21}$$

$$\frac{\mathrm{d}(s\varphi)}{\mathrm{d}t} = \frac{1}{2}(\varphi_{\tilde{\xi}}^2 + \varphi_{\tilde{\eta}}^2). \tag{22}$$

One of the advantages of using the coordinate system $O - \tilde{\xi}\tilde{\eta}$ is that the size of the computation domain and the size of the element used in the numerical simulation can remain roughly the same in the time domain. But these parameters will vary with s in the coordinate system (x, y). As a result, at the initial stage, we have a small domain with small elements in (x, y) . They will increase with time at a rate proportional to s. This is clearly a more rational procedure.

2.4. Calculation of acceleration

The time domain problem is usually solved by the time marching technique. Once the velocity potential is found, Eqs. (21) and (22) can be used to find the surface elevation and the potential on the free surface, respectively. If the body motion is prescribed, the calculation can then move to the next time step. For the body in free fall, the problem becomes rather complicated. Its velocity and position will depend on the acceleration which is not yet known. The acceleration depends on the hydrodynamic force on the body, which in turn depends on the acceleration. The procedure developed by Wu and Eatock Taylor (1996, 2003) is therefore used to decouple this mutual dependence.

When the potential has been found, the Bernoulli equation can be used to obtain the pressure

$$p = -\rho\frac{\partial\phi}{\partial t} - \frac{1}{2}\rho\nabla\phi\nabla\phi, \tag{23}$$

where ρ is the density of the fluid. At each time step, ϕ can be found from the solution of the boundary value problem, but $\partial\phi/\partial t$ is not given explicitly; it may be calculated by the finite difference method using the solution from the last time step but the result is not always accurate. In fact it is often found that when the pressure obtained in this way is used to calculate the body motion, the result is prone to instability. An alternative is to treat $\partial\phi/\partial t$ as another unknown function. It satisfies the Laplace equation and $\partial\phi/\partial t = -0.5\nabla\phi\nabla\phi$, on the free surface. On the wedge surface,

it can be found (Wu, 1998)

$$\frac{\partial \phi_t}{\partial n} = -\dot{V} n_y + V \frac{\partial \phi_y}{\partial n}. \tag{24}$$

Conite et al. (1990) also gave a condition for ϕ_t but with no details. Their result contains the curvature of the body surface. The reason for that is yet to be established. For constant speed ($\dot{V} = 0$), $\partial\phi/\partial t$ can be solved once the potential is known. In general, the solution depends on the unknown acceleration. Thus it can be found only if it is combined with the force.

The hydrodynamic force on the body can be obtained by integrating the pressure over its wetted surface

$$\begin{aligned} F &= \int_{S_0} p n_y \, \mathrm{d}S \\ &= -\rho \int_{S_0} \left(\phi_t + \frac{1}{2} \nabla\phi \nabla\phi \right) n_y \, \mathrm{d}S. \end{aligned} \tag{25}$$

From Newton's law, we have

$$-M_b \dot{V} = F + F_e, \tag{26}$$

where M_b is the body mass and F_e is the external force (the minus sign on the left hand side is because the positive direction of V is opposite to that of y or F). Here the mutual dependence of force and acceleration becomes more evident. To avoid that, we may write

$$\phi_t = -\dot{V} \chi_1 + \chi_2, \tag{27}$$

χ_i satisfies the Laplace equation in the fluid domain and the following boundary conditions:

$$\frac{\partial \chi_1}{\partial n} = n_y, \quad \frac{\partial \chi_2}{\partial n} = V \frac{\partial \phi_y}{\partial n} \tag{28}$$

on the body surface, and

$$\chi_1 = 0, \quad \chi_2 = -0.5(\phi_x^2 + \phi_y^2) \tag{29}$$

on the free surface. On all other boundaries, we have

$$\frac{\partial \chi_i}{\partial n} = 0. \tag{30}$$

Eq. (25) becomes

$$F = \rho \int_{S_0} \left(\dot{V} \chi_1 - \chi_2 - \frac{1}{2} \nabla\phi \nabla\phi) \right) n_y \, \mathrm{d}S. \tag{31}$$

Substituting this into (26), we obtain

$$-(M_b + N)\dot{V} = Q + F_e, \tag{32}$$

where

$$N = \rho \int_{S_0} \chi_1 n_y \, \mathrm{d}S, \tag{33}$$

$$Q = -\rho \int_{S_0} \left(\chi_2 + \frac{1}{2} \nabla\phi \nabla\phi \right) n_y \, \mathrm{d}S. \tag{34}$$

Eq. (32) shows that the acceleration of the body can be obtained directly, once the potential has been found. This can be used in Eq. (27) to obtain $\partial\phi/\partial t$ and as a result the pressure can be found from Eq. (23).

It should be noted that the numerical solution of χ_1 and χ_2 are also obtained in the stretched coordinate system. They both satisfy the Laplace equation in $O{-}\tilde{\xi}\tilde{\eta}$. The boundary conditions can be written as

$$\frac{\partial \chi_1}{\partial n} = n_{\tilde{\eta}}, \quad \frac{\partial \chi_2}{\partial n} = V \frac{\partial \varphi_{\tilde{\eta}}}{\partial n} \tag{35}$$

on the body surface, and

$$\chi_1 = 0, \quad \chi_2 = -0.5(\varphi_{\tilde{\xi}}^2 + \varphi_{\tilde{\eta}}^2) \tag{36}$$

on the free surface.

2.5. Numerical method

The boundary value problems defined in the previous sections, including φ in Sections 2.2 and 2.3, and χ_j in Section 2.4, can be solved by using the complex potential $w = \phi + \mathrm{i}\psi$, where ψ is the stream function. The procedure is similar to that used previously for the nonlinear wave radiation and diffraction problem (Longuet-Higgins and Cokelet, 1976; Lin et al., 1985; Wu and Eatock Taylor, 1995). Cauchy's theorem gives

$$\oint \frac{w}{z - z_0}\,\mathrm{d}z = 0, \tag{37}$$

where $z = x + \mathrm{i}\,y$ and z_0 is a point outside of the fluid domain. The integral in Eq. (37) is along the boundary of R, where we can write

$$w = \sum_{j=1}^{n} w_j N_j(z), \tag{38}$$

w_j are the nodal values of the complex potential and the interpolation function is chosen as

$$N_j(z) = \begin{cases} (z - z_{j+1})/(z_j - z_{j+1}), & z \in (z_j, -z_{j+1}), \\ (z - z_{j-1})/(z_j - z_{j-1}), & z \in (z_{j-1}, z_j), \\ 0 & z \notin (z_{j-1}, z_{j+1}). \end{cases} \tag{39}$$

Substituting Eq. (38) into (37), letting z_0 approach node z_k and using the boundary conditions, and moving the known terms to the right-hand side of the equation while keeping those unknown on the left, we have

$$\sum_{j=1}^{n_2} A_{kj}\phi_j|_{j\in S_0+S_C} + \mathrm{i}\sum_{j=1}^{n_2} A_{kj}\psi_j|_{j\in S_F} = -\sum_{j=1}^{n_2} A_{kj}\phi_j|_{j\in S_F} - \mathrm{i}\sum_{j=1}^{n_2} A_{kj}\psi_j|_{j\in S_0+S_C}, \tag{40}$$

where

$$A_{kj} = \frac{z_k - z_{j-1}}{z_j - z_{j-1}} \ln\frac{z_j - z_k}{z_{j-1} - z_k} + \frac{z_k - z_{j+1}}{z_j - z_{j+1}} \ln\frac{z_{j+1} - z_k}{z_j - z_k}. \tag{41}$$

S_C in Eq. (40) is the boundary at the far field as shown in Fig. 1. The condition imposed there does not have a noticeable effect on the flow near the body if S_C is chosen to be sufficiently far away from the body. Thus it can usually be assumed that $\partial\phi/\partial n = 0$ on S_C. As a result S_C will be a streamline, similar to S_0, on which the stream function is known. On the free surface, the potential at each time step is known based on the boundary condition in Eqs. (5) and (22) and it is therefore moved to the right-hand side of Eq. (40) together with the stream function on S_C and S_0. The potential and stream function on the left-hand side of Eq. (40) are the unknowns to be found.

In summary, the numerical solution starts from the similarity solution in Section 2.2 using the boundary element method discussed above coupled with the analytical solution in the jet. Once the convergence is achieved, the result will be used as the initial solution in Section 2.3 with a very small $s$and the initial entry speed. The time domain simulation will then take over together with procedure in Section 2.4 to calculate the acceleration. Within the jet, the procedure outlined in Section 2.2 cannot be used, as the entry speed is not constant and the flow is not self-similar. It is possible to model fully the jet flow if the mesh used is of sufficiently resolution. But this means a large number of elements, which makes the calculation quite inefficient. It is also possible to have an ill-conditioned matrix when the free surface is very close to the body surface when the jet is very thin. On the other hand, since the pressure in the jet is very close to the atmospheric pressure it has very little direct effect on the body acceleration and deformation. Thus the jet is usually cut in the previous numerical simulations (Zhao and Faltinsen, 1993; Lu et al., 2000). This may not cause too much concern if the entry speed is constant, even though the force history has a spike and the pressure is highly oscillatory near the intersection when the jet is cut. This kind of behaviour will, however, cause a problem here. Therefore, no jet cut is applied in the present work. Instead, because the jet is so thin, the potential on the body surface attached to the jet is obtained directly from the potential on the free surface and the body surface boundary condition. In fact, one can use the Taylor expansion in terms of $\hat{\xi}$ which is in the direction perpendicular to the body surface. As $\partial\phi/\partial\hat{\xi}$ on the body surface is known and ϕ is known on the jet surface, ϕ on the body surface can be found if only the linear term in the Taylor expansion is kept. As a result, both the potential and the stream function become unknown within this part of the body, and they are moved to the right hand side of Eq. (40). This avoids an ill-conditioned matrix. Also, to avoid the inaccuracy in the velocity on the free surface, the component normal to the body surface in the jet zone is assumed to be equal to that of the body surface. After this treatment, in all the simulations undertaken below there is no need to cut the jet and the solution is quite smooth.

3. Experiment

An experiment was conducted at Shanghai Jiaotong University (Sun, 2001) to measure the structural response of a wedge entering water through free fall motion. Both acceleration and strain were recorded. Here we use only the former to validate the numerical simulation.

The set-up of the experiment is shown in Fig. 2. A tank is constructed of glass embedded in a steel frame. The inner dimensions of the tank are 1.65 m in length, 0.8 m in width and 1.45 m in depth. The water depth is 1.1 m. A sliding platform on which the test model is fixed is made of stainless steel. A glass plate is attached to each end of the model to prevent water flowing onto the upper side of the model. A typical model made of ABS (acrylonitrile butadiene styrene) plate is shown in Fig. 3. It is 60 cm long and 20 cm wide. The plate is 3 mm thick for the results provided below although measurement has been made for plates of different thickness. The cross-section of the model is a V-shaped wedge. The Young's modulus E, Poisson Ratio v and the density ρ are measured before test. They are

$$E = 2.65 \times 10^9 \text{ kg/(m s}^2\text{)}, \quad v = 0.387, \quad \rho = 1.060 \times 10^3 \text{ kg/m}^3.$$

Tests are conducted for wedges with different dead-rise angle, entry speed and weight. The last two of these are adjusted by changing the initial height of the model and by adding additional weight to the model. Two YE14127 acceleration sensors, two 2635 charge amplifiers and a HP-VXI data collection and analysis system are used in the experiment to collect and process data. Points A1 and A2 in Fig. 4 are the locations where the data for acceleration is recorded. Their average is used as the acceleration of the body.

It should be noted that there is friction between the sliding platform and the frame. The acceleration of the model is not equal to the acceleration due to gravity, even before the impact occurs. Friction still exists when the body enters water. We may assume that the friction remains the same in both cases. It can then be taken into account in the analysis by using

$$g_e = g - \frac{f}{M_b},$$

Fig. 2. Experiment setup.

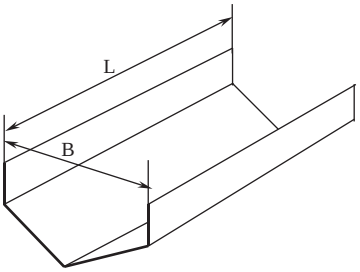

Fig. 3. Model of a V-shaped body.

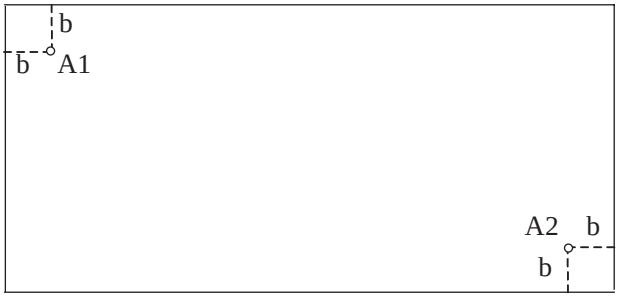

Fig. 4. Positions of acceleration sensors with $b = 3$ cm.

where g_e is the real acceleration of the body before the model touches water, g is the acceleration due to gravity, f is the frictional force and M_b is the total mass of the falling body. As g and M_b are known, and g_e can be measured, f can then be obtained from the equation above. As a result of this procedure, F_e in Eq. (26) can be written as $F_e = -M_b g_e$.

4. Numerical results

We first consider the case of water entry with constant speed, which has been extensively studied as discussed in the introduction. The problem is solved here by both a similarity solution and the time domain simulation. Fig. 5 gives the wave elevation for four different dead-rise angles. The figure shows that the two methods give graphically indistinguishable results. Fig. 6 gives the pressure distribution over the wedge surface, which has been dimensionalized by ρV^2. Good agreement is clearly evident. In particular, with the treatment introduced in the paper, both methods accurately give zero pressure in the long and thin jet. There is no oscillation.

We now consider the cases investigated in the experiment. The element size used in the coordinate system $(\tilde{\xi}, \tilde{\eta})$ is 0.05 and the initial value of s in Eq. (19) is taken as 10^{-4} m, as 10^{-5} m is found to give no visible difference. The time step varies during the simulation and is chosen based on the element size in the coordinate system (x, y). In particular, the time step is chosen to be sufficiently small so that no fluid particle on the free surface would flow across the jet into the body surface in the numerical simulation. Based on these requirements, it has been found the time step at the beginning of the simulation is in the order of 10^{-7}–10^{-8} s, depending on the dead-rise angle.

Fig. 7 gives results for acceleration $a = \dot{V}$ (m/s^2) against time t (s) at $\beta = \pi/4$ with different entry speed V_s, body weight and g_e. The positive value means that the acceleration is the direction of the gravity. It can be seen that the results from the simulation and the experiment are in excellent agreement; but there is some discrepancy at larger time. Part of the reasons for this is because the model was pulled to stop towards the end of the impact. The pulling force from the rope is not included in the simulation. Another important point is the wedge in the experiment is of finite size. The jet will not always stay on the body surface as in the numerical solution. Other factors which may affect the comparison are (i) the end effect in the experiment where the flow is not fully two-dimensional and (ii) the gravity effect on the flow.

Fig. 8 gives results for the acceleration at $\beta = \pi/9$. The comparison is once again fairly good, but the discrepancy is larger than that in the case of $\beta = \pi/4$. In addition to the possible sources of error mentioned above, the air cushion

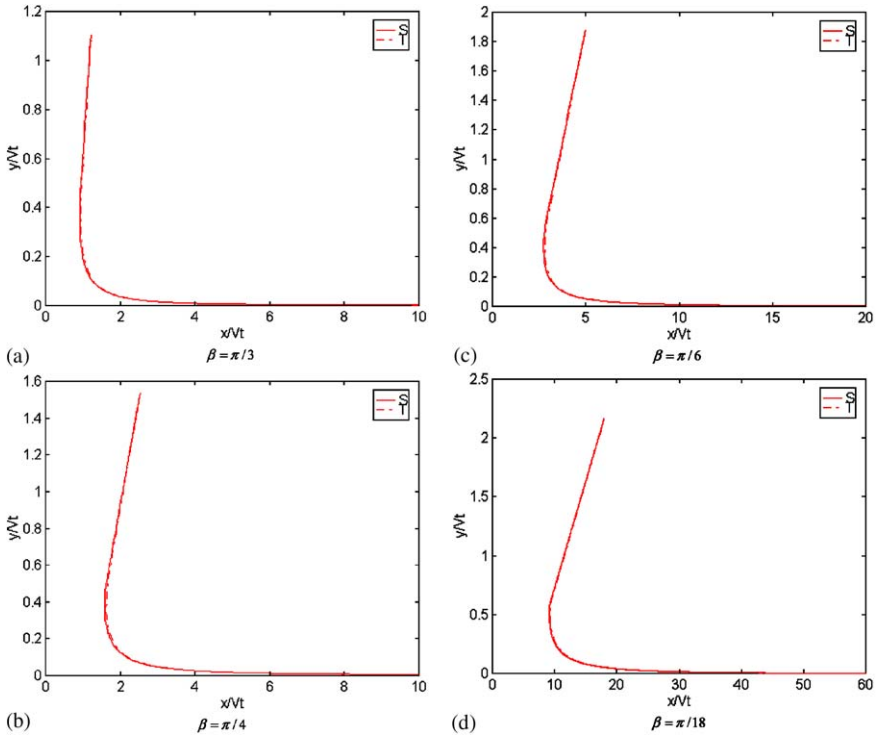

Fig. 5. Comparison of wave elevations at constant entry speed (S: similarity solution, T: time domain solution), (a) $\beta = \pi/3$, (b) $\beta = \pi/4$, (c) $\beta = \pi/6$, (d) $\beta = \pi/18$.

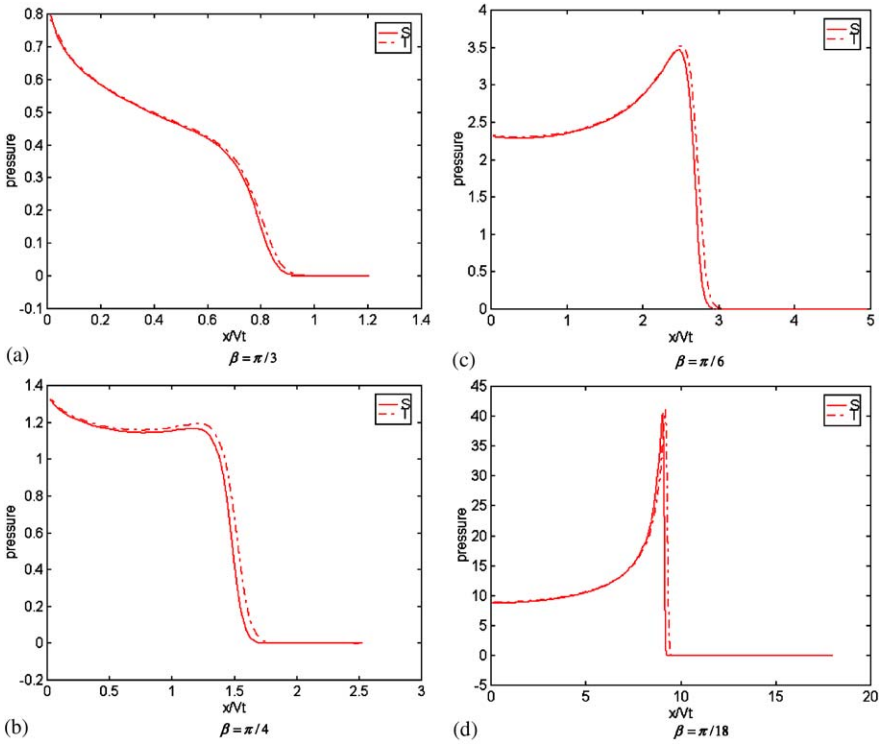

Fig. 6. Comparison of pressure distribution at constant entry speed (S: similarity solution, T: time domain solution), (a) $\beta = \pi/3$, (b) $\beta = \pi/4$, (c) $\beta = \pi/6$, (d) $\beta = \pi/18$.

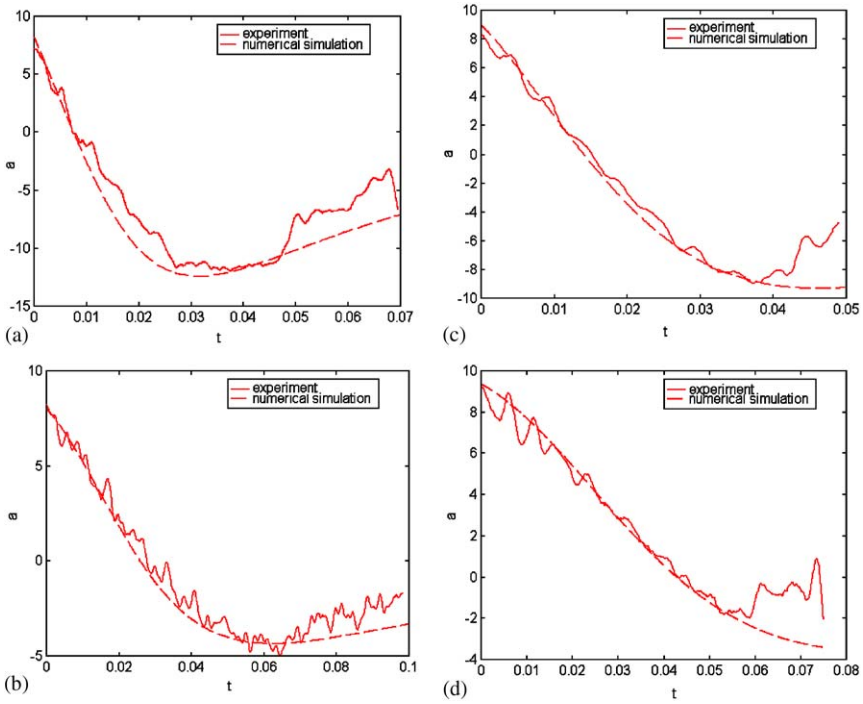

Fig. 7. Acceleration at $\beta = \pi/4$: (a) $g_e = 8.2015\ \mathrm{m/s^2}$, $M_b = 13.522$ kg, $V_s = 1.57974$ m/s, (b) $g_e = 8.0062\ \mathrm{m/s^2}$, $M_b = 13.522$ kg, $V_s = 0.95623$ m/s, (c) $g_e = 8.9716\ \mathrm{m/s^2}$, $M_b = 30.188$ kg, $V_s = 1.69673$ m/s, (d) $g_e = 9.3523\ \mathrm{m/s^2}$, $M_b = 30.188$ kg, $V_s = 1.03634$ m/s.

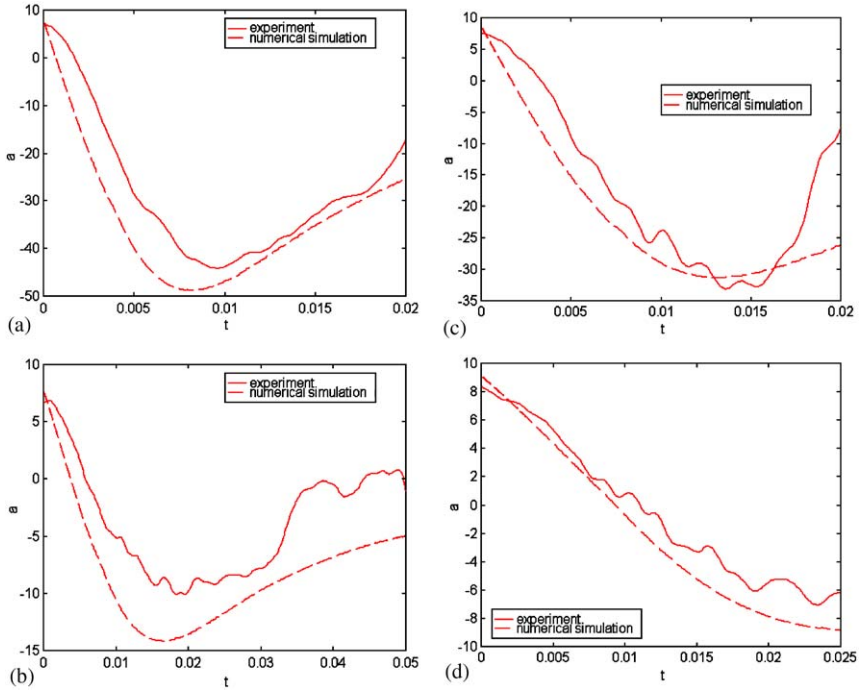

Fig. 8. Acceleration at $\beta = \pi/9$: (a) $g_e = 7.9228\ \mathrm{m/s^2}$, $M_b = 13.492$ kg, $V_s = 1.54405$ m/s, (b) $g_e = 7.8144\ \mathrm{m/s^2}$, $M_b = 12.952$ kg, $V_s = 0.86165$ m/s, (c) $g_e = 8.6103\ \mathrm{m/s^2}$, $M_b = 29.618$ kg, $V_s = 1.54405$ m/s, (d) $g_e = 9.1091\ \mathrm{m/s^2}$, $M_b = 29.618$ kg, $V_s = 0.85462$ m/s.

effect usually becomes more important at smaller dead-rise angle. This effect may not only change the acceleration g_e just before the wedge enters the water, but may also lead to some bubbles being trapped in the liquid after the body has entered the water. Another possible reason for the larger discrepancy in Fig. 8 is that at smaller β the jet will pass the top of the wedge much earlier, as the velocity of the jet is much faster. It should also be mentioned that the entry speed is obtained from the integration of the measured acceleration and its accuracy will have important an effect on the result. With all these imperfections, the comparison between the numerical simulation and the experimental data is nevertheless quite good.

5. Conclusions

The hydrodynamic problem of a wedge entering water through free fall motion has been analysed numerically and experimentally. The comparison between the results from the simulation and the measured data is quite good. Although some of the techniques used here, such as the similarity solution and shallow water approximation, are well established, they have been successfully used in a new context. The success of this work is also largely due to the use of the stretched coordinate system in the time domain and the introduction of the auxiliary function to decouple the mutual dependence of the hydrodynamic force and the body acceleration. All these have laid a good foundation for tackling more general problems, such as the case of a body with curvature and oblique entry.

Acknowledgements

This work is partly supported by the Royal Society of UK and the National Science Foundation of China through a joint project between UCL and SJTU over the period of 1997-2000, to which the authors are most grateful.

References

Cointe, R., 1991. Free-surface flows closes to surface-piercing body. In: Miloh, T. (Eds.), Mathematical Approaches in Hydrodynamics, Society for Industrial and Applied Mathematics, Phàladelphia pp. 319–334.

Cointe, R., Geyer, P., King, B., Molin, B., Tramoni, M., 1990. Nonlinear and linear motions of a rectangular barge in a perfect fluid. In: Proceedings of 18th Symposium of Naval Hydrodynamics, National Academy Press, ONR, Washington.

Dobrovol'skaya, Z.N., 1969. On some problems of similarity flow of fluid with a free surface. Journal Fluid Mechanics 36, 805–829.

Faltinsen, O.M., 2002. Water entry of a wedge with finite dearrise angle. Journal of Ship Research 46, 39–51.

Fraenkel, L.E., McLeod, J.B., 1997. Some results for the entry of a blunt wedge into water. Philosophical Transactions of the Royal Society of London A355, 523–535.

Greenhow, M., 1987. Wedge entry into initially calm water. Applied Ocean Research 9, 214–223.

Howison, S.D., Ockendon, J.R., Wilson, S.K., 1991. Incompressible water-entry problems at small dead-rise angles. Journal of Fluid Mechanics 222, 215–230.

Iafrati, A., Korobkin, A.A., 2002. Hydrodynamic loads at the early stage of a floating wedge impact, 17th Workshop on Water Waves and Floating Bodies, Cambridge, UK.

Iafrati, A., Carcaterra, A., Ciappi, E., Campana, E.F., 2000. Hydroelastic analysis of a simple oscillator impacting the free surface. Journal of Ship Research 44, 278–289.

Korobkin, A.A., Wu, G.X., 2000. Impact on a floating circular cylinder. Proceedings of the Royal Society of London A456, 2489–2514.

Lin, W.M., Newman, J.N., Yue, D.K., 1985. Nonlinear forced motions of floating bodies. In: Proceeding of 15th Symposium of Naval Hydrodynamics, National Academy Press, ONR, Washington.

Longuet-Higgins, M.S., Cokelet, E.D., 1976. The deformation of steep surface waves on water: I. A numerical method of computation. Proceedings of the Royal Society of London A350, 1–26.

Lu, C.H., He, Y.S., Wu, G.X., 2000. Coupled analysis of nonlinear interaction between fluid and structure during impact. Journal of Fluids and Structures 14, 127–146.

Mei, C.C., 1983. The Applied Dynamics of Ocean Surface Waves. Wiley-Interscience, New York.

Mei, X., Liu, Y., Yue, D.K.P., 1999. On the water impact of general two-dimensional sections. Applied Ocean Research 21, 1–15.

Sun, H., 2001. Fluid–structure interaction during free water entry of two dimensional wedge. MSc Thesis, Department of Engineering Mechanics, Shanghai Jiaotong University, China.

Wu, G.X., 1998. Hydrodynamic force on a rigid body during impact with liquid. Journal of Fluids and Structures 12, 549–559.

Wu, G.X., 2001. Initial pressure distribution due to jet impact on a rigid body. Journal of Fluids and Structures 15, 365–370.

Wu, G.X., Eatock Taylor, R., 1995. Time stepping solution of the two dimensional nonlinear wave radiation problem. Ocean Engineering 22, 785–798.

Wu, G.X., Eatock Taylor, R., 1996. Transient motion of a floating body in steep waves. 11th Workshop on Water Waves and Floating Bodies, Hamburg, Germany.

Wu, G.X., Eatock Taylor, R., 2003. The coupled finite element and boundary element analysis of nonlinear interactions between waves and bodies. Ocean Engineering 30, 387–400.

Zhao, R., Faltinsen, O., 1993. Water entry of two-dimensional bodies. Journal of Fluid Mechanics. 246, 593–612.